



## **Investigation of Fiber Length Differences in Distributed MIMO Sigma-Delta-over-Fiber Systems**

Downloaded from: <https://research.chalmers.se>, 2024-07-22 17:57 UTC

Citation for the original published paper (version of record):

Olofsson, F., Karlsson, M., Eriksson, T. et al (2023). Investigation of Fiber Length Differences in Distributed MIMO Sigma-Delta-over-Fiber Systems. 49th European Conference on Optical Communications (ECOC 2023). <http://dx.doi.org/10.1049/icp.2023.2400>

N.B. When citing this work, cite the original published paper.

# Investigation of Fiber Length Differences in Distributed MIMO Sigma-Delta-over-Fiber Systems

Frida Olofsson<sup>(1)</sup>, Magnus Karlsson<sup>(1)</sup>, Thomas Eriksson<sup>(2)</sup>, Christian Fager<sup>(1)</sup>

<sup>(1)</sup>Department of Microtechnology and Nanoscience, Chalmers University of Technology, Gothenburg, Sweden, [frida.olofsson@chalmers.se](mailto:frida.olofsson@chalmers.se)

<sup>(2)</sup>Department of Electrical Engineering, Chalmers University of Technology, Gothenburg, Sweden,

**Abstract** *The effect of having different fiber length to each access point in distributed MIMO is experimentally investigated through testbed experiments. It is found that the delay differences can severely degrade the performance of the system. A method for compensating the delay effect is proposed.*

## Introduction

Distributed (D-MIMO) is an emerging technique where multiple carefully coordinated wireless access points (APs) are spatially distributed. This results in improved communication performance compared to the co-located MIMO (C-MIMO) technique commonly used today<sup>[1]</sup>. D-MIMO is also essential for realizing cell-free massive MIMO, a promising technology for future mobile networks<sup>[2]</sup>. To provide simultaneous service to multiple users, MIMO systems use channel state information to perform beamforming. As beamforming relies on that signals from several APs combine constructively at the users, the APs have to be precisely RF-phase synchronized. For C-MIMO this can be done in a conventional way using a common clock at the AP, but for D-MIMO systems this is not feasible. Instead, D-MIMO systems often ensure phase synchronization by doing frequency up-conversion centrally, using Analog-Radio-over-Fiber (ARoF) or Sigma-Delta-over-Fiber (SDoF)<sup>[3]</sup>. Several D-MIMO demonstrations using optical fiber connected APs with central frequency upconversion have been reported. In<sup>[4]</sup> a test-bed based on SDoF consisting of 12 APs serving two users was presented. In<sup>[5]</sup>, real-time  $2 \times 2$  MU-MIMO using SDoF to distribute the APs was presented. In<sup>[6]</sup>, 2 APs based on ARoF were presented and evaluated.

However, these demonstrations all assume a symmetrical system where fibers of equal length are used to distribute the signals, no matter the distance to the central unit (CU) where the joint processing is done. In a real implementation the fiber links connecting to different APs can be of different length, which will introduce different time delays between the transmit branches. These time-delays are usually several times larger than

the ones introduced in the wireless paths and can therefore not be handled by the conventional D-MIMO signal processing techniques alone. In<sup>[7]</sup>, the effect of different fiber lengths was addressed for D-MIMO systems using ARoF and OFDM modulation. It was found that, for a fiber length difference larger than 100 meters the data throughput fell quickly. However, the effect when using SDoF and single-carrier modulation has not yet been addressed, neither has a solution for length differences beyond 100 meters been proposed.

In this paper we use a SDoF testbed with two APs to investigate how fiber length differences affect the channel estimate and beamforming performance in a single-carrier D-MIMO wireless system. Furthermore, we propose a method to compensate for the impact of the fiber length difference.

## Sigma-Delta-over-Fiber testbed

The testbed used in the experimental investigations is shown in Figure 1 and presented in more detail in<sup>[4]</sup>. The CU consists of a PC and an FPGA where a baseband data signal is digitally upconverted to a RF-carrier frequency of 2.35 GHz. Bandpass sigma-delta modulated RF-signals are distributed in binary form over a standardized 10 Gbits/s SFP+ optical fiber link<sup>[8]</sup>. At the APs, the signals are converted back to electrical domain, recovered with a bandpass filter, amplified and transmitted over-the-air with patch antennas. Two APs are used in this demonstration, but the testbed can support up to 12 APs<sup>[4]</sup>. A signal an-

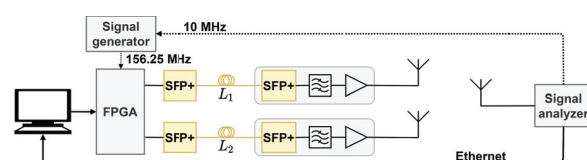


Fig. 1: Schematic of the setup used in the measurements.

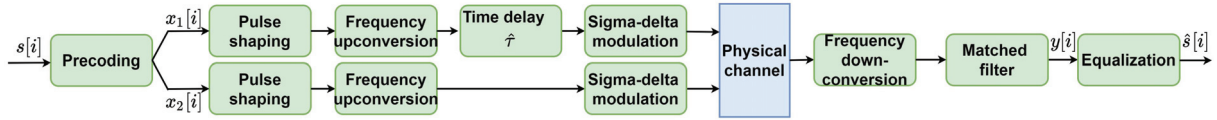


Fig. 2: Block diagram of the system model.

alyzer (Keysight, N9030A) with an identical patch antenna is used as a receiver, thus acting as a user equipment. During the experiments, the PC and the signal analyzer are connected via Ethernet. A signal generator (Rohde& Schwarz, SMU200A) with output frequency 156.25 MHz, phase locked to the signal analyzer with a 10 MHz reference clock, is used as input clock to the FPGA. AP<sub>1</sub> and AP<sub>2</sub> are connected to the CU with fibers of length  $L_1$  and  $L_2$ , respectively.  $L_1$  and  $L_2$  can be altered in order to change the fiber length difference.

### System model

A block diagram of the applied signal processing steps can be seen in Figure 2. Although the single-user case is considered here, it can easily be extended to several users. In the transmitter, single-carrier 16-QAM symbols are generated, with symbol rates from 20 MSym/s to 60 MSym/s. Channel estimation is done using time-orthogonal pilots, and the communication symbols are precoded with the maximum ratio transmission precoder<sup>[9]</sup>. The precoder is designed to create one signal per transmit branch, which will combine constructively at the receiver. The symbols are upsampled and pulse shaped using a root-raised cosine filter with roll-off factor 0.2, and digitally upconverted to a center frequency of 2.35 GHz. The difference in fiber length is compensated for, by delaying the signal that propagates in the shortest fiber with a time delay  $\hat{\tau}$ . Finally, a fourth order bandpass sigma-delta modulation is applied to the RF-signal. The received signal  $y$  at time index  $[i]$  can be described by

$$y[i] = \sum_{k=1}^K \sum_{m=0}^M h_{km} x_k[i-m] + z[i], \quad (1)$$

where  $K$  is the number of transmit branches, and  $M$  is the channel memory length.  $h_{km}$  is the impulse response of the channel between the user and transmit branch  $k$ .  $x_k$  is the input to each transmit branch and  $z$  is the added noise. The symbols  $s[i]$  relates to  $x_k$  as  $x_k = p_k s$ , where  $p_k$  is the precoder coefficient of branch  $k$ .

In the receiver, the signal is downconverted, downsampled and matched filtered. Thereafter,

an equalizer with  $J$  taps is applied on the received communication symbols. Based on the received symbols,  $y$ , the equalizer creates a least-square estimate  $\hat{s}$  of the transmitted symbols  $s$ , according to

$$\hat{s}[i] = \sum_{j=0}^J g_j y[i-j], \quad (2)$$

where  $g_j$  are the equalizer coefficients. The equalizer partially compensates for the channel memory effects in (1). However, it can never recover the beamforming gain achieved as the signals from the two transmit branches arrive phase aligned at the receiver and combine constructively.

### Investigation of time delay difference

Investigations were done to define and compensate for the time-delay  $\tau$  induced by differences in fiber length. Note that  $\tau$  is defined as the actual delay difference between the fibers and  $\hat{\tau}$  the applied delay used to compensate for it. During the studies, a fixed fiber length difference was used, with  $L_1 = 15$  m and  $L_2 = 60$  m. The number of taps in the equalizer was set to  $J = 10$ , as it was sufficient to compensate for intersymbol interference for equal fiber lengths. Two methods were then used to estimate  $\tau$ . Firstly,  $\hat{\tau}$  was swept from  $0.21 \mu\text{s}$  to  $0.24 \mu\text{s}$ , and the error vector magnitude (EVM) of the received symbols was calculated, see Figure 3(a). A minimum was found corresponding to  $\tau \approx 0.224 \mu\text{s}$ . Secondly, the same signal was transmitted simultaneously into the fibers links, and the output signals from the two APs were captured by an oscilloscope with equal length cables. The time-delay difference was detected and averaged over 10 measurements, resulting in a time delay of  $\tau \approx 0.225 \mu\text{s}$ . Finally, the results were compared to approximating the time delay based on the speed of the signal and the physical length difference between the fibers, assuming a typical refractive index value of  $n = 1.5$ . This resulted in  $\tau = 0.225 \mu\text{s}$ , which corresponds well to the two measured values of  $\tau$ . The approximation  $\tau \approx n\Delta L/c_0$ , where  $n$  is the group index and  $c_0$  the vacuum light velocity, was therefore used in the following measurements when  $\Delta L = L_2 - L_1$  was altered.

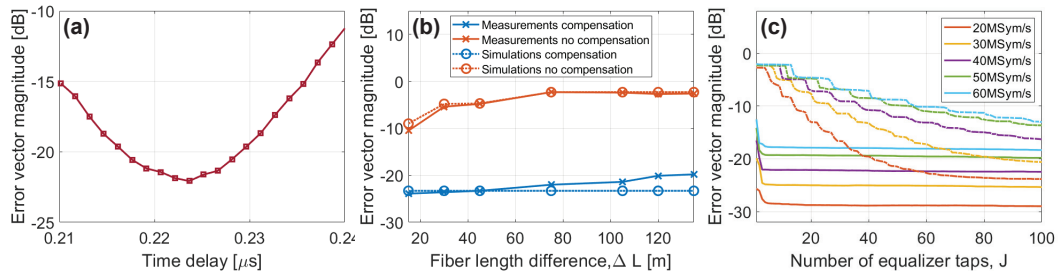


**Fig. 3:** (a) Measurements of Error vector magnitude vs time-delay compensation,  $\hat{\tau}$ , for 45 m length difference. (b) Measurements and simulations of Error vector magnitude versus fiber length difference, with and without time delay compensation, number of taps  $J = 10$ . (c) Measurements of Error vector magnitude versus number of equalizer taps  $J$  for different symbol rates, when including the time delay compensation  $\hat{\tau}$  (solid) and when not including the time delay compensation  $\hat{\tau}$  (dashed).

Measurements were then performed sweeping  $\Delta L$ , with a fixed  $L_1 = 15$  m and different  $L_2 = \{30, 45, 60, 90, 120, 150\}$  m. The effect of  $\tau$  was investigated by applying the processing steps described in Figure 2, with and without including the delay block  $\hat{\tau}$ . The symbol-rate was fixed at 40 MSym/s, and the number of taps was set to  $J = 10$ . In Figure 3(b), it is seen that even for small  $\Delta L = 15$  m, EVM is much higher when not including  $\hat{\tau}$ . This was compared to simulations, and a close similarity for the case without  $\hat{\tau}$  could be noted. When including  $\hat{\tau}$ , the measurements also agree well with simulations, apart from a small decrease for the measurements when increasing  $\Delta L$ . This could be caused by a decrease in optical power due to larger fiber attenuation causing a slight optical SNR degradation at the optical receiver.

The constellation diagrams of the received symbols for  $\Delta L = 45$  m are presented in Figure 4(a). It can clearly be seen that the result degrades significantly when not doing the time-delay compensation. Furthermore, the relative phase between the channel estimates  $h_1$  and  $h_2$  for 100 subsequent measurements are presented in Figure 4(b), where it can be seen to be very unstable when not doing time-delay compensation.

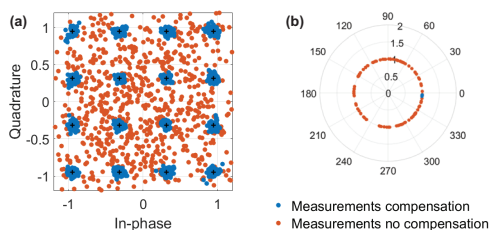


**Fig. 4:** (a) Constellation diagram when including (blue) and not including (red)  $\hat{\tau}$ . (b) Relative phase between branch 1 and 2 when including (blue) and not including (red)  $\hat{\tau}$ .

### Investigation of equalizer based compensation

As  $\tau$  increases, adjacent symbols will start to interfere, which to some extent can be handled by

the equalizer. It is, therefore, interesting to see if there is a limit on how much of the intersymbol interference the equalizer can compensate for. To investigate this, measurements with and without  $\hat{\tau}$  were done, and the number of equalizer taps  $J$  were swept. The fiber length difference was fixed at  $\Delta L = 45$  m and five different communication signal bandwidths were measured. In Figure 3(c) it can be seen that, when not including delay compensation  $\hat{\tau}$  many more taps are needed in the equalizer to decrease EVM. It can also be noted that a considerable difference in EVM remains, even after equalization with  $J = 100$  taps. This is consistent with theory, as a perfect equalizer can adjust for the intersymbol interference, but not recreate the beamforming gain. When increasing  $J$ , discrete steps can be seen for all measurements. For the measurements without including  $\hat{\tau}$  the width of steps correspond exactly to the fiber length difference in number of taps. Therefore it is reasonable to see an improvement when including exactly the same number of taps that the time delay is in terms of number of symbols.

### Conclusion

In summary, this work has investigated how different fiber lengths affect the beamforming performance in a D-MIMO system. The result shows that, even small fiber length differences degrade the wireless communication performance significantly. Moreover, it is shown that an equalizer with a large number of taps can to some extent compensate for the intersymbol interference occurring, but not recover the beamforming gain. Furthermore, a time-delay compensation method is proposed, which is shown to recover the performance irrespective of the fiber length difference.

### Acknowledgements

This work was funded by the Swedish Research Council (grant VR-2019-05174).

## References

- [1] S. Zhou, M. Zhao, X. Xu, J. Wang, and Y. Yao, "Distributed wireless communication system: A new architecture for future public wireless access", *IEEE Communications Magazine*, vol. 41, no. 3, pp. 108–113, 2003. DOI: 10.1109/MCOM.2003.1186553.
- [2] J. Zhang, S. Chen, Y. Lin, J. Zheng, B. Ai, and L. Hanzo, "Cell-free massive mimo: A new next-generation paradigm", *IEEE Access*, vol. 7, pp. 99 878–99 888, 2019. DOI: 10.1109/ACCESS.2019.2930208.
- [3] F. Olofsson, L. Aabel, M. Karlsson, and C. Fager, "Comparison of transmitter nonlinearity impairments in externally modulated sigma-delta-over fiber vs analog radio-over-fiber links", in *2022 Optical Fiber Communications Conference and Exhibition (OFC)*, 2022, pp. 1–3.
- [4] I. C. Sezgin, M. Dahlgren, T. Eriksson, *et al.*, "A low-complexity distributed-mimo testbed based on high-speed sigma-delta-over-fiber", *IEEE Transactions on Microwave Theory and Techniques*, vol. 67, no. 7, pp. 2861–2872, 2019. DOI: 10.1109/TMTT.2019.2904265.
- [5] C.-Y. Wu, H. Li, O. Caytan, *et al.*, "Distributed multi-user mimo transmission using real-time sigma-delta-over-fiber for next generation fronthaul interface", *Journal of Lightwave Technology*, vol. 38, no. 4, pp. 705–713, 2020. DOI: 10.1109/JLT.2019.2947786.
- [6] D. Pérez-Galacho, D. Sartiano, and S. Sales, "Fronthaul links based on analog radio over fiber", in *2019 European Conference on Networks and Communications (EuCNC)*, 2019, pp. 475–478. DOI: 10.1109/EuCNC.2019.8802030.
- [7] Y. Fan, A. E. Aighobahi, N. J. Gomes, K. Xu, and J. Li, "Performance analysis of commercial multiple-input-multiple-output access point in distributed antenna system", *Opt. Express*, vol. 23, no. 6, pp. 7500–7513, Mar. 2015. DOI: 10.1364/OE.23.007500.
- [8] L. Pessoa, J. Tavares, D. Coelho, and H. Salgado, "Experimental evaluation of a digitized fiber-wireless system employing sigma delta modulation", *Optics Express*, vol. 22, Jul. 2014. DOI: 10.1364/OE.22.017508.
- [9] T. Lo, "Maximum ratio transmission", *IEEE Transactions on Communications*, vol. 47, no. 10, pp. 1458–1461, 1999. DOI: 10.1109/26.795811.